Faraday Discussions

Bond Dissociation Energies of Lignin-Carbohydrate Complexes

Journal:	*Faraday Discussions*
Manuscript ID	FD-ART-04-2025-000045.R1
Article Type:	Paper
Date Submitted by the Author:	09-Jun-2025
Complete List of Authors:	Elder, Thomas; USDA Forest Service Southern Research Station, Lawoko, Martin; KTH Royal Institute of Technology, Fiber and Polymer Technology

ARTICLE

Bond Dissociation Energies of Lignin-Carbohydrate Complexes

Thomas Elder,*[a] Martin Lawoko [b]

Received 00th January 20xx,
Accepted 00th January 20xx

DOI: 10.1039/x0xx00000x

Lignin-carbohydrate complexes, in which lignin and polysaccharides are directly connected have been identified and extensively analyzed. To date, however, the origin of these structures has not been unequivocally established. That notwithstanding, it has been found that delignification, whether by conventional pulping and bleaching processes or in the biorefinery context is effected by the presence of lignin-carbohydrate complexes. Using density functional theory calculations, the current work has evaluated the thermodynamics of bond dissociation as a function of structure and chemical composition. Among the lignin-carbohydrate complexes that have been identified, the homolytic bond dissociation energy is highest for the α-benzyl ethers and γ-ester, with phenyl glycosides being markedly less endothermic. This is consistent with observations on recalcitrance of these compounds. Heterolytic cleavage reactions of the α-benzyl ethers are less endothermic, due to water solvation of the ions. The latter observation may provide support for the proposed homolytic cleavage reaction, since if heterolysis were operative, the α-benzyl ethers would not exhibit the level of recalcitrance that is observed experimentally.

Introduction

Despite extensive work, questions still remain about the presence of covalent connections between lignin and polysaccharides, in lignin-carbohydrate complexes. While these moieties have been identified, and mechanisms for their formation proposed, it is still unclear if they occur naturally or are artifacts of processing or the isolation methods[1–3]. This has been addressed experimentally by examinations of extracellular lignin and dehydrogenation polymers modified with galacturonic acid or water soluble xylans, resulting in the detection of lignin-carbohydrate bonds by NMR analysis, indicating that their formation may occur in the cell wall independent of the isolation method[2]. Isolation methods have been extensively described and include ball-milling, enrichment of lignin-carbohydrate complexes by enzymatic and acid/base hydrolysis and sequential fractionation[1]. Among these, the sequential extraction method has the advantage that the structure of the carbohydrates is preserved, due to the absence of hydrolysis as affected by the other methods. This notwithstanding, sequential extraction typically involves multiple steps and a variety of solvents and conditions, such that it is not a trivial process.

Structures that have been proposed for lignin-carbohydrate complexes are, phenyl glucosides, alpha-ethers and gamma-esters (Figure 1), in which the carbohydrates in question are the hemicelluloses[1,3]. The main secondary cell wall hemicelluloses, are galactoglucomannans in conifers, glucuronoxylans in angiosperms and glucuronoarabinoxylans in grasses[4].

[a] *USDA-Forest Service, Southern Research Station, Auburn, AL, USA.*
[b] *Fiber and Polymer Technology, Wallenberg Wood Science Center, Royal Institute of Technology, Stockholm, Sweden Address here.*
Supplementary Information available: . See DOI: 10.1039/x0xx00000x

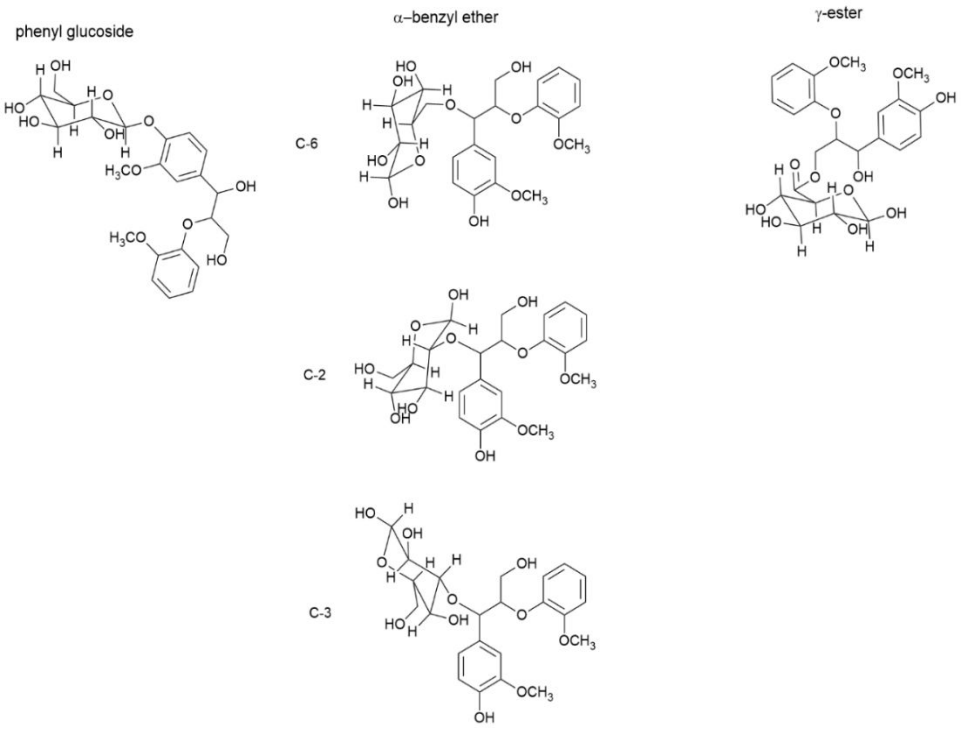

Figure 1. Lignin-carbohydrate complex

Uncertainties regarding the origin of lignin-carbohydrate complexes notwithstanding, such linkages have been implicated in the processing of lignocellulosics.

The kraft pulping process removes a large proportion of the lignin present in the original wood, but to achieve acceptable levels of brightness, subsequent bleaching steps are required to degrade the residual lignin. Lignin-carbohydrate complexes, their presence and structure have been investigated to account for this residual lignin. In some of the initial work on this, the presence of ether bonds between carbohydrates was reported that were stable in alkali[5]. Subsequently, in the oxygen delignification of softwood, results showed that lignin complexed to xylan was resistant to delignification, whereas galactan complexes could be removed[6]. Residual lignin in softwood that had been subjected to kraft pulping and oxygen delignification was found to be rich in lignin-carbohydrate complexes. At high kappa numbers, lignin was connected to xylan, while with higher levels of delignifcation, glucomannan linkages were predominant[7]. Using an enzymatic fractionation method, on spruce, eucalyptus and birch, lignin-carbohydrate complexes were completely recovered but less so for the hardwoods probably due to higher content of β-O-4 linkages. Furthermore, differences between the lignin-carbohydrate complexes of the hardwoods were detected[8]. In work on a number of commercially important hardwood species, higher syringyl-guaicyl ratios increased the delignification rate while the presence of lignin-carbohydrate complexes was proposed to account lower levels of delignification[9]. In contrast to results from softwoods, the lignin-carbohydrate complexes identified after kraft pulping of birch were mainly xylan linked, while the glucomannan-lignin complexes were decreased[10].

Lignin-carbohydrate complexes have also been reported in sulfite pulps. Spruce sulfite pulp was found to have three lignin-carbohydrate complexes, one of which has a low lignin content and is attached to glucans, while two others with higher lignin content involved glucomannan and a xylan-lignin-glucomannan network. Benzyl ether linkages are proposed for these, and the preponderance of xylan-lignin complexes is thought to be due to the lower reactivity of xylan towards acid hydrolysis, for which a mechanism has been proposed[11,12]. In pine heartwood, lignin complexes were also found with xylan and glucomannans, with γ-esters and α-ethers detected, the latter of which are not present in resultant sulfite pulp. The presence of such lignin-carbohydrate complexes may impede sulfite pulping[13]. The production of dissolving pulp from pine heartwood occurs in a sequence of reactions, in one of which, γ-ester, α-ether and phenyl glycoside lignin-carbohydrate complexes are degraded leading to greater solution of lignin[12].

The effect of lignin-carbohydrate complexes within the context of the biorefinery has been reviewed by Zhao and co-workers[14]. It is discussed that lignin-carbohydrate complexes can inhibit ethanol production from biomass, impact the economics of the biorefinery and that analyses on both composition and molecular geometry are needed. Furthermore, the clean isolation of lignin and hemicelluloses is generally impeded, requiring secondary extraction steps. In contrast, an alternative to the “conventional” biorefinery has been proposed in

which lignin-carbohydrate complexes are specifically retained and isolated for use in value-added products such as emulsifiers for lignin nanoparticles and pharmaceutical applications[15]. The process involves an initial hydrothermal treatment, followed by acetone extraction to generate a lignin-carbohydrate fraction. The properties of the lignin-carbohydrate complexes, including the carbohydrate percentage which is thought to influence their properties, is varied by varying the liquid/solid ratio and the severity of the process.

Given that the economically feasible operation of a biorefinery depends on the full utilization of all components of biomass for high-value products, a "consolidated biorefinery" has been proposed in which the structure of hemicelluloses and lignin are relatively unchanged[16]. The process involves an initial hydrothermal treatment with subcritical water at 160°C followed by extraction with ethanol-water. The hemicelluloses and lignin are separated in the first step, while the second step protects the isolated lignin from condensation[17]. It has been found that the hydrothermal treatment has little effect on the quantity of lignin-carbohydrate complexes, which are mostly represented by benzyl ethers and γ-esters, while phenyl glycosides are removed, such that the former are thought to control hemicellulose retention. It is concluded that the reactivity, or lack thereof, of the lignin-carbohydrate complexes are important factors in hemicellulose recalcitrance[18]. Among these, it has been concluded that benzyl ethers exhibit the highest levels of recalcitrance followed by γ-esters and phenylglycosides[19]. Furthermore, at 160°C under neutral to slightly acid conditions, lignin models undergo homolytic cleavage reactions[20,21]. Finally, under mild conditions of temperature and pH, the extraction of spruce yielded lignin-carbohydrate complexes composed of arabinoglucuronoxylans and galactoglucomannans, with the presence of benzyl ethers and phenylglycosides detected[22].

In addition to the documented effects on delignification, the biological activity of lignin-carbohydrate complexes, including antioxidant , antitumor and antiviral properties, along with ultraviolet and immune system activity have been reviewed recently[23]. In work on lignin-carbohydrate complexes isolated from bamboo, all extracts exhibited antioxidant properties, with lignin-rich fractions performing better than carbohydrate-rich fractions[24]. Extracts from spruce, exhibited performance consistent with those from bamboo, albeit with lower activity[25]. Reports on lignin-carbohydrate complexes from wheat straw have found that extracts from sheath tissue was more active than material from leaves or stalks and that extraction with LiCl/DMSO improves radical scavenging performance[26,27]. It would be of interest to explore structure-activity relationships of lignin-carbohydrate complexes with respect to biological activity.

From the foregoing it is evident that lignin-carbohydrate complexes are factors in the processing of lignocellulose, which can be predicated on the separation of the components. It will also be observed that the nature of the lignin-carbohydrate complex is dependent on the substrate from which it is isolated and the method by which it is isolated. Given the effect of these lignin-carbohydrate complexes on industrial applications, the objective of the current paper is concerned with the thermodynamics associated with the homolytic cleavage of bonds between lignin models and carbohydrates as a function of linkage type (phenyl glycoside, benzyl ether or ester), the sugar involved and the position on the sugar through which the bond occurs. This will be accomplished by the performance of density functional theory calculations on lignin-carbohydrate models and the products of the cleavage reactions. Density functional theory calculations have been successfully and extensively applied to lignin model compounds to determine the energetics of reactions associated with degradation and formation of lignin-based structures[28–34].

Results and Discussion

α-benzyl ethers

Examples of the structure of the α-benzyl ethers are shown in Figure 2. These are variable and do not seem to correlate with carbohydrate substituent, stereochemistry of the lignin model dimer or methoxyl content. Most of the complexes exhibit an extended conformation as shown in Figure 2a. There are, however instances in which stacked conformations are found as in Figures 2b and 2c. In the former, the stacking is between the aromatic rings, while the latter is between the carbohydrate and one of the aromatic rings. These conformations are indicative of π-π and π-σ interactions.

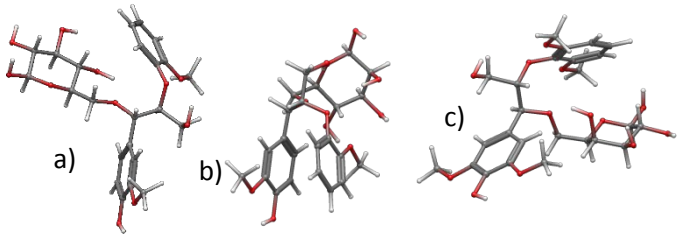

Figure 2. Example of α-benzyl ethers in a) extended, b) stacked (aromatic-aromatic), c) stacked (aromatic-carbohydrate conformations

The reactions of the α-benzyl ethers under consideration are shown in Figure 3.

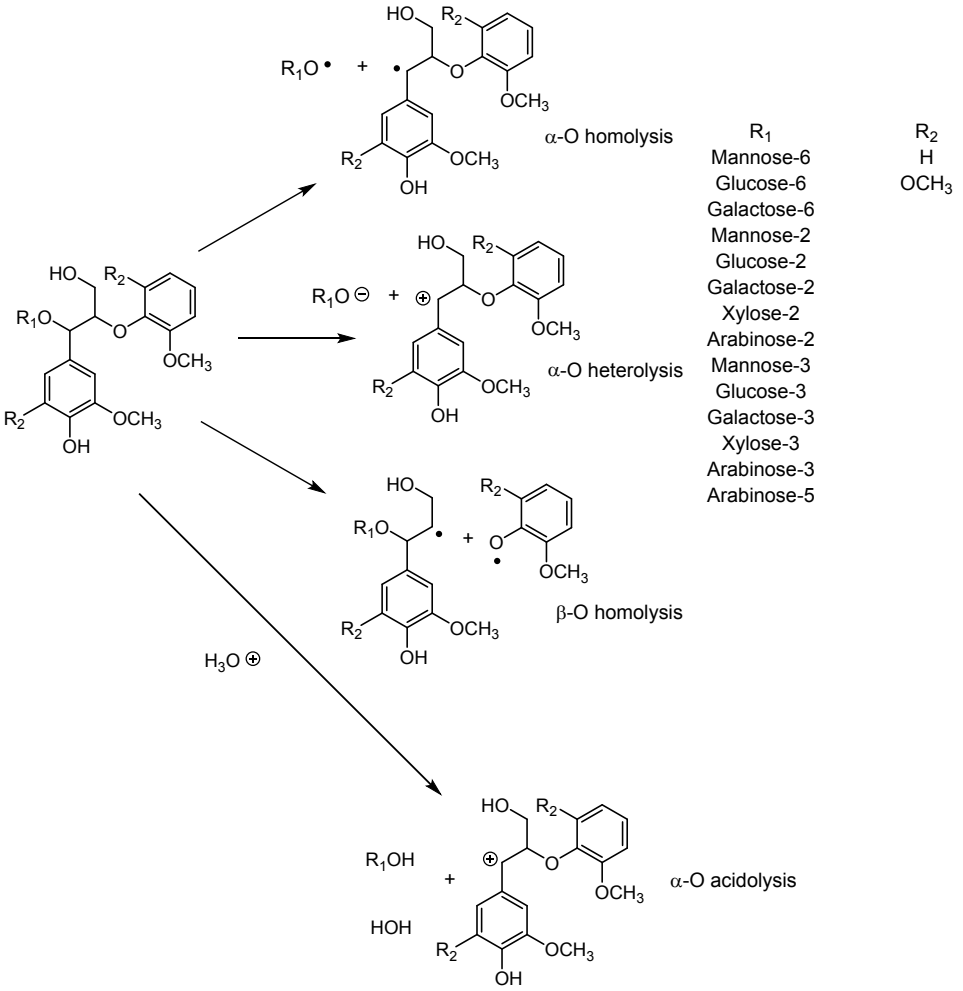

Figure 3. Reactions of α-benzyl ethers

Calculations were performed for both RS/SR (*erythro*) and RR/SS (*threo*) stereoisomers of the lignin fragment, but as in Berstis et al. there were no discernible patterns or consistent differences due to stereochemistry, such that for the purposes of these results, the energies of reaction reported here are an average of the two stereoisomers[35]. The bond dissociation energies reported are from enthalpy calculations at 1 atmosphere and 298.15 K, with water solvation.

α-O homolysis

The bond dissociation energies for the homolytic cleavage of the α-O bond for the guaiacyl and syringyl models are shown in Figure 4. The average bond dissociation energies were very similar at 80.1 and 80.6 kcal mol^{-1}, for the guaiacyl and syringyl models, respectively. It will be noticed that for these and the subsequent ethers, cleavage could potentially occur on either side of C-O-C bond. The reaction energies reported throughout are the lower of these, which are generally ~30 kcal mol^{-1} less endothermic and therefore much more likely to occur. These results are consistent with another recent study on the energetics of lignin-carbohydrate complexes [36]. The values ranged from 77.9-81.9 and 78.3-83.3 kcal mol^{-1}, for guaiacyl and syringyl, respectively. These values are somewhat more endothermic than reported for bonds between flavonoids and monolignols[33]. Sorting by substitution position and sugar results in the plots in Figure 5. From these it can be seen that the bond dissociation energies of the syringyls are generally higher as are the complexes formed through C-2 and C-3. Among the sugars, mannose substitution exhibits the highest bond dissociation energy, xylose and galactose are similar and intermediate, while glucose is lower. Arabinose substitution results in variable bond dissociation energy. These observations, notwithstanding, it should be borne in mind that the differences in bond dissociation energies for these reactions are, other than at the extremes, relatively small. From a kinetic standpoint, homolytic reactions are barrierless, such that the bond dissociation energy is taken as the activation energy, to which

rate constants have an exponential relationship[37]. As a consequence, small differences in bond dissociation energy can translate into much larger differences in reaction rate.

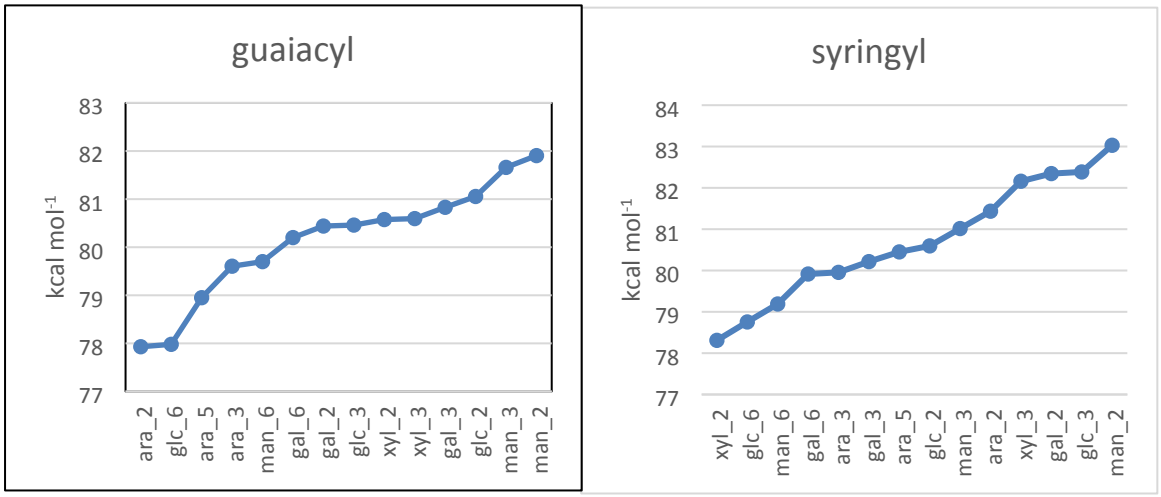

Figure 4. Homolytic bond dissociation energies of α-benzyl ethers

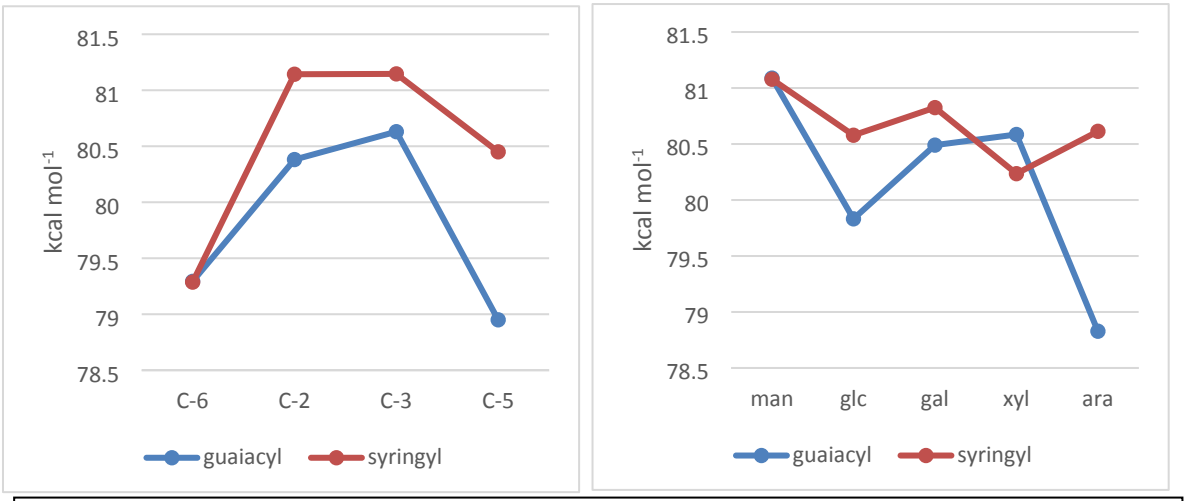

Figure 5. Homolytic bond dissociation energies of α-benzyl ethers sorted by position and sugar

α-heterolysis

The bond dissociation energies for the heterolytic cleavage of the α-benzyl ethers are shown in Figure 6. The average values are 64.4 and 66.1 kcal mol^{-1}, with ranges of 49.4-71.0 and 62.0-69.6 for the guaiacyl and syringyl complexes, respectively, substantially less endothermic than the homolytic reactions. The average values are, as expected, lower than the corresponding homolytic cleavage, since these calculations were done with water solvation which stabilizes ions. Furthermore, the ranges are larger than for the homolytic cleavage reactions. Sorting by the position through which the substitution occurs (Figure 7) shows that C-6 has the highest bond dissociation energy, differing by about 3 kcal mol^{-1} with C-2 and C-3. Substitution through C-5, which only occurs with arabinose is consistently the lowest. Sorting by sugar (Figure 7), the guaicyl complexes exhibit a monotonic decrease in bond dissociation energy with mannose>glucose>galactose>xylose>arabinose, while there is variation with the mannose substituted syringyl model. It is interesting to note that, as in the homolytic cleavage reactions, the highest bond dissociation energy continues to involve mannose substitution. For both lignin models, the least endothermic values are dominated by the pentose-based complexes.

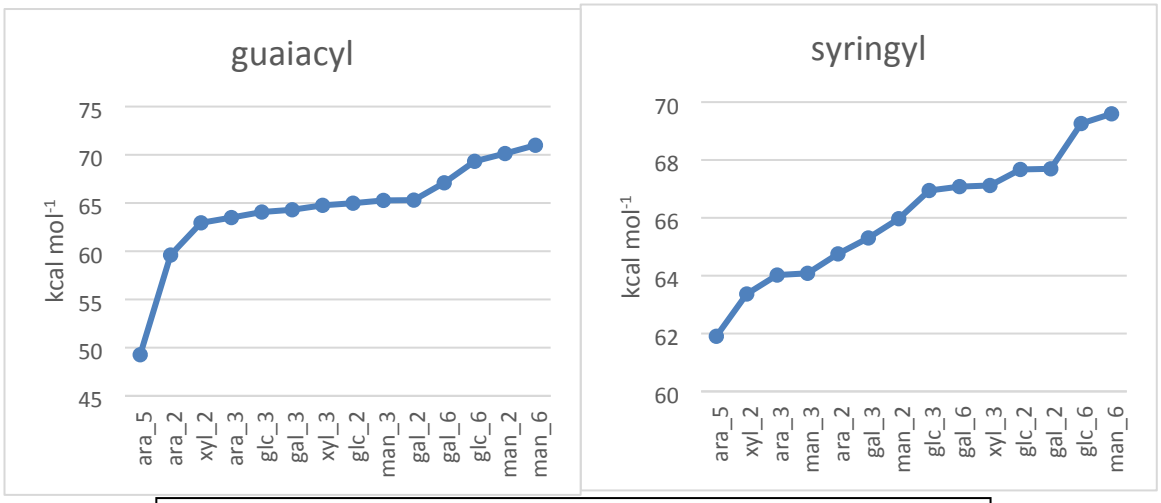

Figure 6. Heterolytic bond dissociation energies of α-benzyl ethers

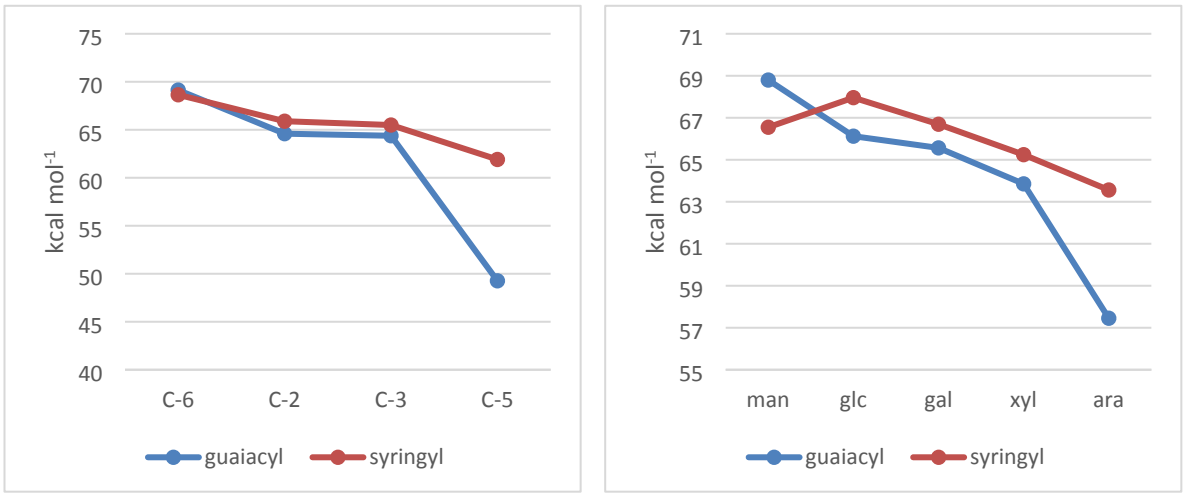

Figure 7. Heterolytic bond dissociation energies of α-benzyl ethers sorted by position and sugar

β-O homolysis

Although this reaction does not directly involve the reactivity of the lignin-carbohydrate complex that is the objective of the current work, it was evaluated for the sake of completeness and shows that these homolytic reactions are markedly less endothermic than the α-O cleavage. This is due to the stability of the lignin-based products, in which extensive delocalization of the unpaired electron occurs. The bond dissociation energies for the homolytic cleavage of the β-O bonds are as shown in Figure 8. These average 65.1 and 63.9 kcal mol^{-1} with ranges of 64.0-68.4 and 61.5-67.2 kcal mol^{-1} for the guaiacyl and syringyl complexes, respectively. As seen previously, the highest value is associated with mannose substitution. Sorting by position (Figure 9) again reveals that substitution through C-6 has the highest bond dissociation energy and the C-5 is variable. The results from sorting by sugar (Figure 9) vary between guaiacyl and syringyl. The trend of the former is similar to the α-O homolytic cleavage, with mannose substitution being the most endothermic and arabinose substitution the lowest. These values are consistent with those reported for dimeric lignin models[38].

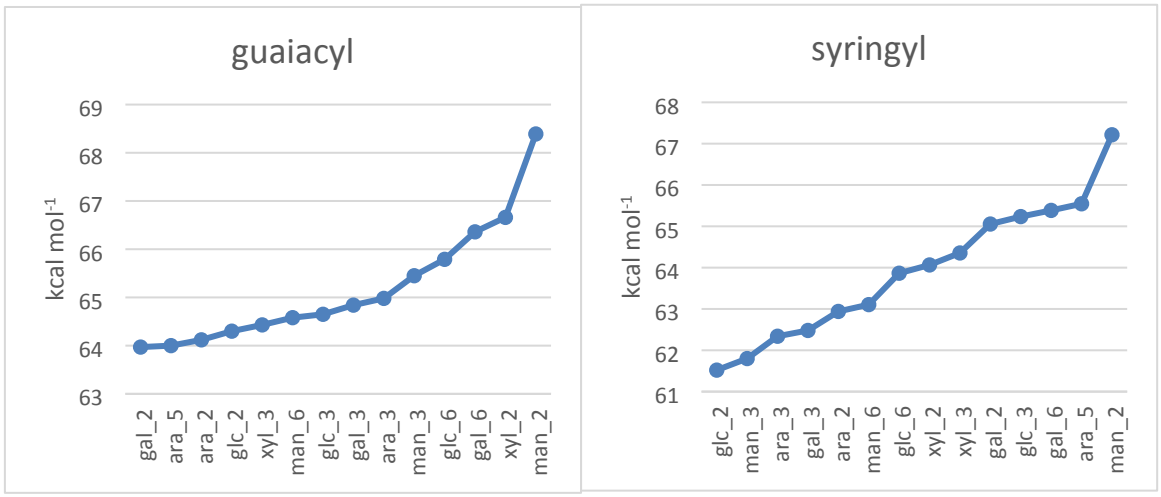

Figure 8. Bond dissociation energies of β-homolysis reactions of α-benzyl ethers

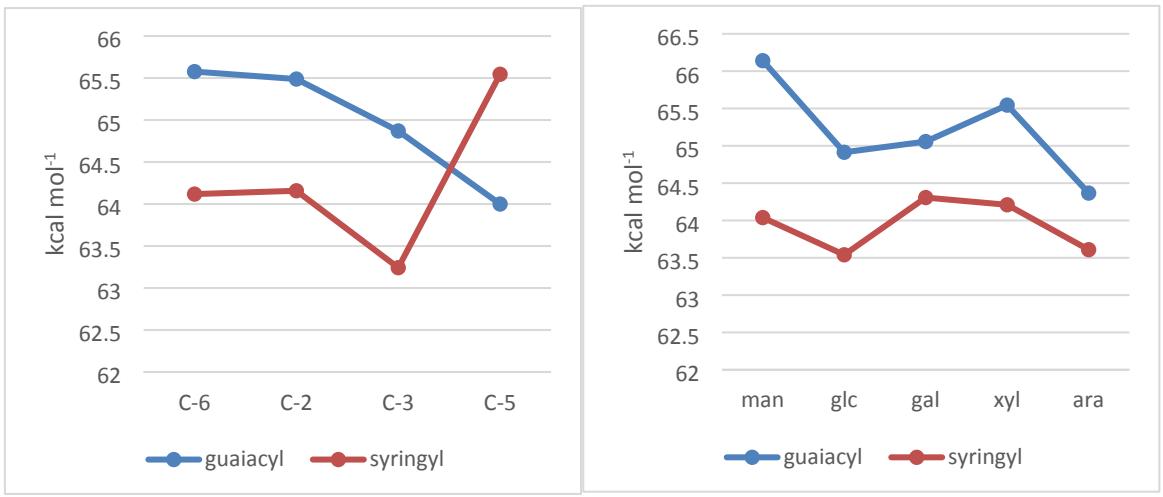

Figure 9. Bond dissociation energies of β-homolysis reactions of α-benzyl ethers, sorted by position and sugar

α-O acidolysis

The acidolysis reactions are considerably less endothermic than those discussed thus far, averaging 16.6 and 17.8 kcal mol^{-1} with ranges of 13.6-19.1 and 15.6-19.9 kcal mol^{-1} for the guaiacyl and syringyl complexes, respectively (Figure 10). This is due to the fact that bonds are both broken and formed in this reaction, rather than a single cleavage as in the previous results. Sorting by position and sugar yields mixed results, but among the sugars, mannose substitution of the guaiacyl complexes continues to give the most endothermic reaction energies (Figure 11).

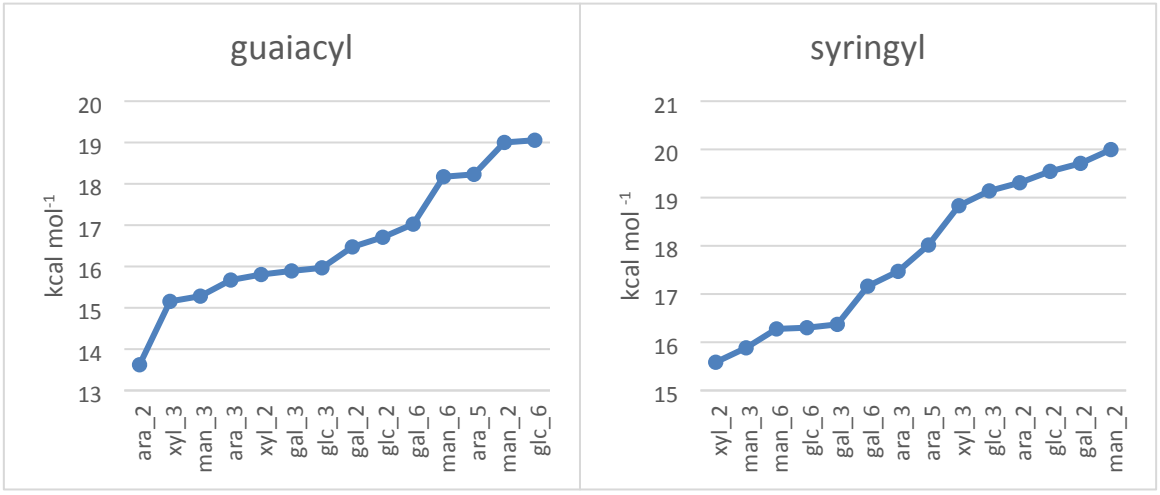

Figure 10. Bond dissociation energies of α-O acidolysis reactions of α-benzyl ethers

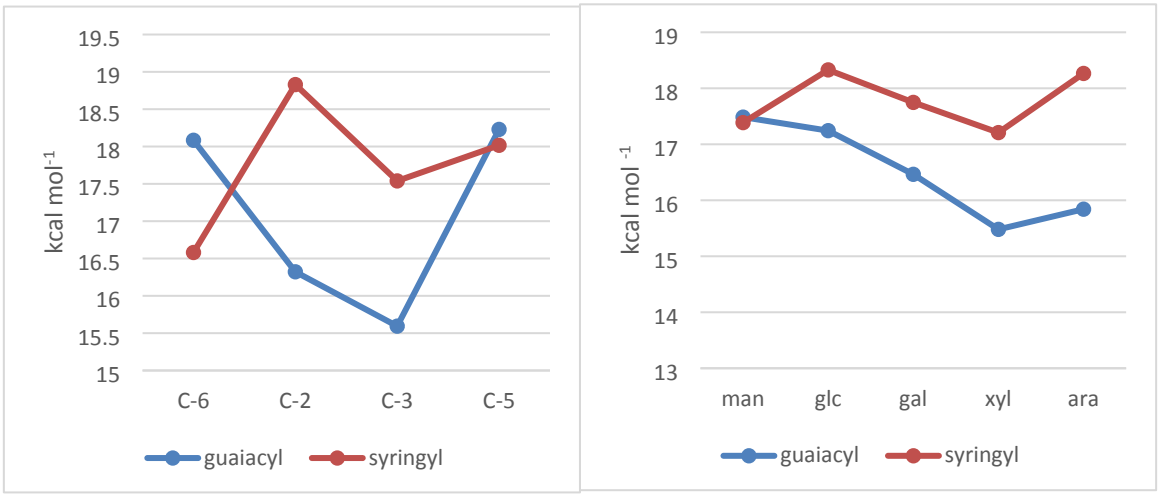

Figure 11. Bond dissociation energies of α-O acidolysis reactions of α-benzyl ethers sorted by position and sugar

Phenylglycosides

Example structures for the phenylglycosides are shown in Figure 12. The conformations for Figure 12a and 12b have stacked and t-shaped conformations, respectively, both of which involve π-π interactions. Figure 12c is a more extended conformation.

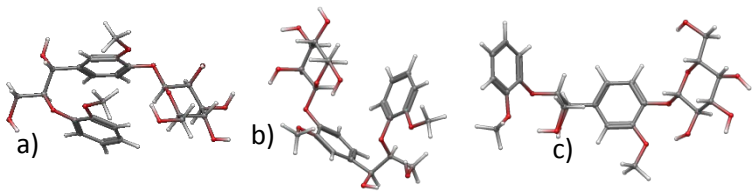

Figure 12. Examples of phenyglycoside structure exhibiting a) aromatic stacked, b) aromatic t-shaped and c) extended conformations

The reactions of the phenylglycosides are as shown in Figure 13 and the bond dissociation energies are shown in Figure 14. Among these the syringyl complexes generally have a lower bond dissociation energy with an average value of 62.3 kcal mol^{-1} in contrast to 64.6 kcal mol^{-1} for the guaiacyl compounds, both of which are much less endothermic than the homolytic cleavage reactions of the α-O benzyl ethers. With the exception of the arabinose-based complex, sugar substitution seems to have an opposite effect, depending on the lignin substituent. As previously observed for the β-O homolysis reactions, the lower endothermicity of these reactions can be attributed to the stability of the lignin-based product and the electron delocalization therein.

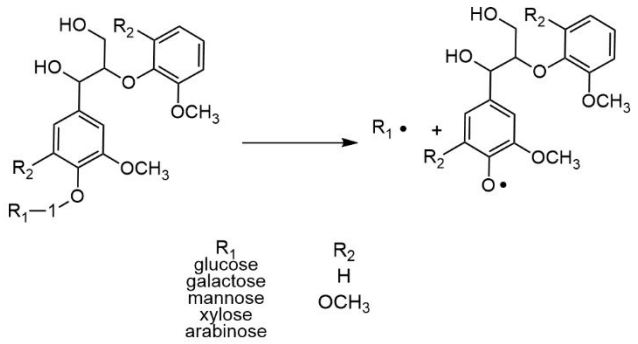

Figure 13. Reactions of phenylglycosides

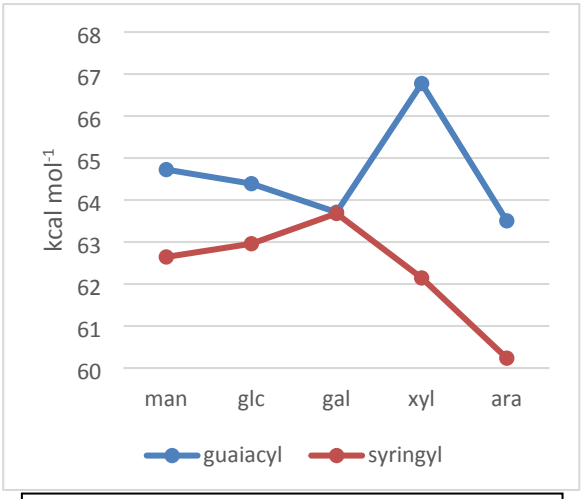

Figure 14. Bond dissociation energies of homolysis of phenylglycosides

γ-esters

The structures for the γ-glucuronoesters are shown in Figure 15. The γ-ester of the syringyl erythro stereoisomer is in an extended conformation, while for the others, the glucuronate group is perpendicular for the aromatic ring, and may therefore be involved in π-σ interactions.

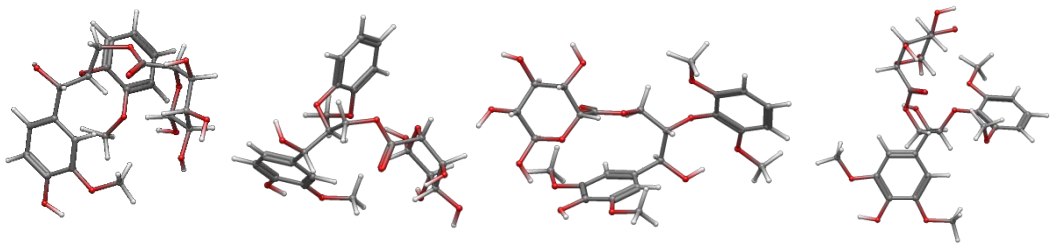

a) b) c) d)

Figure 15. Structures of a) guaiacyl-threo, b) guaiacyl-erythro, c) syringyl-threo, d) syringyl-erythro, γ-glucuronate esters

The homolytic cleavage reaction the of γ-glucuronates is shown in Figure 16. The bond dissociation energies are 79.1 and 78.8 kcal mol^{-1} for guaiacyl *threo* and *erytho*, respectively and 78.6 and 80.7 kcal mol^{-1} for syringyl, *threo* and *erytho*, respectively. Albeit for limited data, the *erytho* stereoisomers have slightly higher bond dissociation energies.

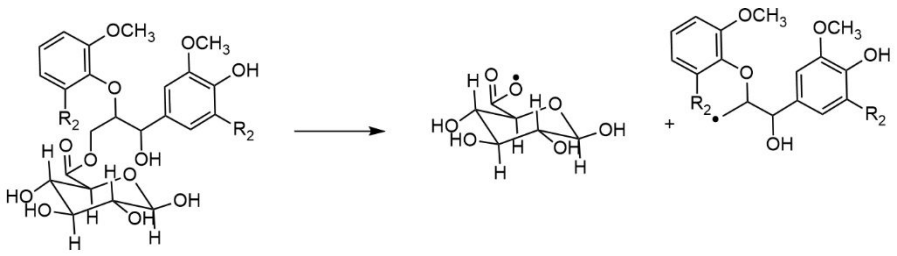

Figure 16. Homolytic cleavage reactions of γ-esters

Carbohydrates

As previously, for comparison purposes, the reaction energies of the carbohydrates have also been determined. The reactions evaluated are as in Figure 17. All structures were disaccharides in which D-pyranose glucose, galactose, mannose and xylose dimers were β-1-4 linked. The arabinose-xylose dimer consisted of L-arabinofuranose with an α-1-3 linkage to D-xylopyranose. The galactose-mannose dimer was D-galactopyranose connected to D-mannopyranose through a β-1-6 linkage. The homolytic cleavage reactions were reasonably constant with high bond dissociation energies between 85 and 95 kcal mol^{-1} (Figure 18). As has been seen previously, due to stabilization of the ions in solution, the heterolytic reactions (Figure 18) have consistently lower bond dissociation energies. Heterolytic 2 exhibits relatively little variability with the carbohydrate composition, while heterolytic reaction 2 changes markedly depending on the sugar moiety. With respect to the latter, the hexose disaccharides (glucose-glucose and mannose-mannose) have similar energies of reaction as do the pentoses (xylose-xylose and arabinose-xylose). The presence of galactose (galactose-mannose and galactose-galactose) results in quite different energies of reaction, possibly due to the axial configuration at C-4. The homolytic cleavage reactions between the carbohydrates are somewhat higher than those α-benzyl ethers and γ-esters, but the heterolytic reaction energies are generally similar.

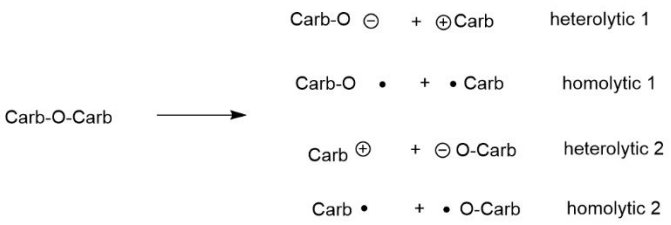

Figure 17. Reactions of dimeric carbohydrates

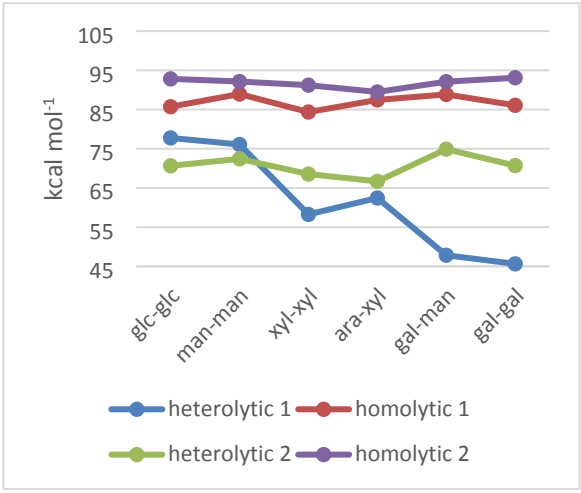

Figure 18. Bond dissociation energies of dimeric carbohydrates

Per the introductory comments, lignin-carbohydrate complexes are found in the residual lignin from various processing methods, even at high-levels of delignification. From the calculations performed in the current work, the homolytic bond dissociation energies of α-benzyl ethers and the γ-esters of glucuronic acid are both ~80 kcal mol^{-1}. In contrast, the bond dissociation energy of the β-O bond in these complexes is ~65 kcal mol^{-1}. Based on this, the bond between lignin and carbohydrate is considerably less reactive than the bond to a subsequent lignin unit and may account for the presence of lignin-carbohydrate complexes even with extensive lignin removal. In addition, as discussed in kraft pulping studies with subsequent oxygen delignification, glucomannan linked lignin-carbohydrate complexes were prevalent[7]. In agreement with this, the current work has found that, in many cases, the least reactive complexes were linked to mannose.

In work on biorefinery applications, benzyl ethers and γ-esters have been reported to be the prevalent lignin-carbohydrate complexes, with a concomitant reduction on phenylglycosides.[17,18] These results are consistent with the bond dissociation energies found in this work. Per the previous comments, the enthalpies for the homolytic cleavage reactions of ethers and esters are ~80 kcal mol^{-1}, while the reactions of the phenylglycosides are considerably less endothermic at ~60 kcal mol^{-1}. As such these thermodynamic differences may explain the experimental observations.

It has been proposed that homolytic cleavage reactions occur at 160°C under neutral to slightly acid conditions [20,21]. It will be noted, however, that results from this work show that, among the α-benzyl ethers, heterolytic cleavage at ~65 kcal mol^{-1}, is less endothermic than homolysis. This value is comparable with that found for the phenylglycosides, such that if a heterolytic cleavage mechanism were operative, it would be expected that the α-benzyl ethers would be similarly degraded and not be present in the proportions observed experimentally. As such, this conclusion supports the hypothesis that degradation is due to homolytic cleavage.

In the isolation of lignin-carbohydrate complexes from sulfite pulps, it has been found that after pulping, α-ethers are not detected and it is proposed that under acidic conditions α-benzyl ether bonds may be broken, leading to sulfonation[12]. The enthalpies of reaction found in the current work, indicate that this reaction is considerably less endothermic than either homolytic or heterolytic cleavage, such that under specific conditions, it could readily occur.

Experimental

Computational details

The work flow for the calculations is as shown in Figure 19..

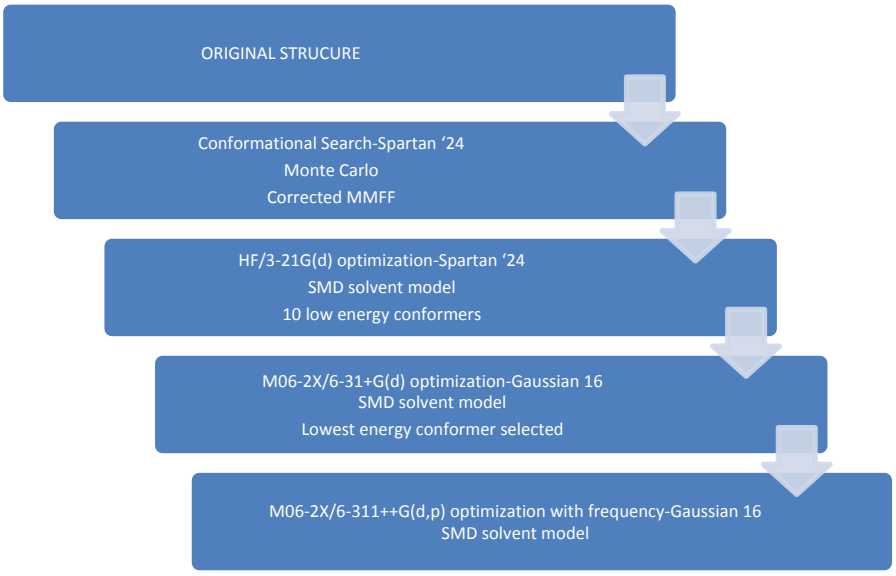

Figure 19. Work flow for calculations

Due to the presence of numerous single bonds within the linkages of the reactants a large number of conformers may result. In order to address this a Monte Carlo conformational search was performed with minimization using the corrected MMFF force-field as implemented in Spartan '24. Based on the unique conformations identified an intermediate optimization was done using Hartree-Fock calculations with water solvation with the SMD solvation model, also within Spartan '24[39]. The 10 lowest energy conformations from the *ab initio* calculations were further refined with the M06-2X density functional theory method, the 6-31+G(d) basis set, the GD3 empirical dispersion correction and SMD solvation with water. Lastly, the lowest energy conformation from the previous step was optimized with the M06-2X

density functional theory method, the 6-311++G(d,p) basis set, the GD3 empirical dispersion correction, SMD solvation with water, and a frequency calculation to insure the identification of an energetic minimum and for determination of thermal corrections. The density functional theory calculations were done using Gaussian 16[40]. The homolytic and heterolytic reaction products were generated by deleting the appropriate bond, and optimization of the resulting doublets or anion/cation pair with the M06-2X density functional theory method, the 6-311++G(d,p) basis set, the GD3 empirical dispersion correction, the SMD solvation with water, and a frequency calculation to insure the identification of an energetic minimum and for determination of thermal corrections. This approach has been used in previous work with lignin adducts[33]. It allows for relaxation with bond cleavage to the closest local minimum. The values reported in this work are enthalpies in kcal mol^{-1} calculated at 1 atmosphere pressure and 289.15 K. Similarly, beginning from the optimized reactant geometry, the acidolysis products were separately optimized without additional conformational searching.

Conclusions

The current results help to account for the reactivity, or lack thereof, that is observed experimentally for lignin-carbohydrate complexes. The relative stability of α-benzyl ethers and γ-esters is consistent with experimental observations such as would be encountered under neutral conditions in the proposed "consolidated biorefinery". The calculations are also in agreement with work on pulping processes. The corresponding homolysis reaction of the β-O bond is markedly less endothermic, showing that lignin could be removed to a large extent, leaving the less reactive intact. There are not large differences or discernible patterns between the individual sugar substituents or the position through which they are connected to the lignin groups. The exception to this generalization is that lignin-carbohydrate complexes formed through mannose substitution are fairly consistent in being the least reactive. As such, no definitive differences with substitution can be reported at this point. With respect to methoxy content, the α-benzyl ether syringyl models are generally more stable for both homolytic and heterolytic cleavage, while reactions involving the β-O group and the phenylglycosides the syringyl models are less stable. The latter may be interpreted as being consistent with the generally higher reactivity of hardwoods over softwoods. The separation between syringyl and guaiacyl based models, however, are small.

Based on this work, further investigations on larger lignin-carbohydrate models, even at the density functional level of theory, could be undertaken to further elucidate relationships between structure and reactivity, and explore the reduction of endothermicity of the α-benzyl ether bond, perhaps through structural modification, alternative reactants or process changes.

Author contributions

TE, conceptualization, investigation, methodology, formal analysis, writing-original draft. ML, conceptualization, investigation, formal analysis, writing-review and editing.

Conflicts of interest

There are no conflicts to declare.

Data availability

The data supporting this article, cartesian coordinates for the lignin-carbohydrate complexes, have been included as part of the Supplementary Information.

Acknowledgements

This work was made possible in part by a grant for high-performance computing resources and technical support from the Alabama Supercomputer Authority. This research was supported in part by the U.S. Department of Agriculture, U.S. Forest Service.

References

1 N. Giummarella, Y. Pu, A. J. Ragauskas and M. Lawoko, *Green Chemistry*, 2019, **21**, 1573–1595.

2 N. Giummarella, M. Balakshin, S. Koutaniemi, A. Kärkönen and M. Lawoko, *J Exp Bot*, 2019, **70**, 5591–5601.

3 O. M. Terrett and P. Dupree, *Curr Opin. Biotechnol,* 2019, **56,** 97-104.

4 H. V. Scheller and P. Ulvskov, *Annu Rev Plant Biol*, 2010, **61**, 263–289.

5 T. Iversen and S. Wännström, *Holzforschung,* 1986, **40**, 19-22.

6 S. Fu and L. A. Lucia, *Ind Eng Chem Res*, 2003, **42**, 4269–4276.

7 M. Lawoko, R. Berggren, F. Berthold, G. Henriksson and G. Gellerstedt, *Holzforschung*, 2004, **58**, 603–610.

8 G. Henriksson, M. Lawoko, M. E. E. Martin and G. Gellerstedt, *Holzforschung*, 2007, **61**, 668–674.

9 R. B. Santos, H. Jameel, H.-M. Chang and P. W. Hart, *Bioresources*, 2013, **8**, 158-171.

10 R. Deshpande, L. Sundvall, H. Grundberg, M. Lawoko and G. Henriksson, *Tappi J*, 2020, **19**, 447–460.

11 M. Lawoko, G. Henriksson and G. Gellerstedt, *Holzforschung*, 2006, **60**, 162–165.

12 R. Deshpande, N. Giummarella, G. Henriksson, U. Germgård, L. Sundvall, H. Grundberg and M. Lawoko, *Ind Crops Prod*, 2018, **115**, 315–322.

13 R. Deshpande, L. Sundvall, H. Grundberg, G. Henriksson and M. Lawoko, *Ind Crops Prod*, 2022, **177**, 114391.

14 Y. Zhao, U. Shakeel, M. Saif Ur Rehman, H. Li, X. Xu and J. Xu, *J Clean Prod,* 2020, **253**, 120076.

15 D. Tarasov, P. Schlee, A. Pranovich, A. Moreno, L. Wang, D. Rigo, M. H. Sipponen, C. Xu and M. Balakshin, *Green Chemistry*, 2022, **24**, 6639–6656.

16 M. Karlsson, N. Giummarella, P. A. Lindén and M. Lawoko, *ChemSusChem*, 2020, **13**, 4666–4677.

17 M. Karlsson and M. Lawoko, *iScience*, 2023, **26**, **107507**.

18 N. Giummarella and M. Lawoko, *ACS Sustain Chem Eng*, 2017, **5**, 5156–5165.

19 A. Martínez-Abad, N. Giummarella, M. Lawoko and F. Vilaplana, *Green Chemistry*, 2018, **20**, 2534–2546.

20 S. Li, K. Lundquist and U. Westermark, *Nord Pulp Paper Res J*, 2000, **15**, 205–210.

21 U. Westermark, B. Samuelsson and K. Lundquist, *Res Chem Intermed,* 1995, **21**, 343-352.

22 N. Giummarella, L. Zhang, G. Henriksson and M. Lawoko, *RSC Adv*, 2016, **6**, 42120–42131.

23 W. Pei, P. Wang, X. Shen, X. Meng, L. Zheng, B. Guo and C. Huang, *ACS Sustain Chem Eng,* 2024, **12**, 14952-14967.

24 C. Huang, S. Tang, W. Zhang, Y. Tao, C. Lai, X. Li and Q. Yong, *ACS Sustain Chem Eng*, 2018, **6**, 12522–12531.

25 Y. Zhang, S. Wang, W. Xu, F. Cheng, A. Pranovich, A. Smeds, S. Willför and C. Xu, *ACS Sustain Chem Eng*, 2019, **7**, 1447–1456.

26 D. Xie, T. Gan, C. Su, Y. Han, Z. Liu and Y. Cao, *Int J Biol Macromol*, 2020, **161**, 315–324.

27 C. Su, T. Gan, Z. Liu, Y. Chen, Q. Zhou, J. Xia and Y. Cao, *Int J Biol Macromol*, 2021, **184**, 369–379.

28 J. M. Younker, A. Beste and A. C. Buchanan, *Chem Phys Lett*, 2012, **545**, 100–106.

29 T. Elder, *Energy & Fuels*, 2014, **28**, 1175–1182.

30 T. Elder, *Energy & Fuels*, 2013, **27**, 4785–4790.

31 T. Elder, J. C. del Río, J. Ralph, J. Rencoret and H. Kim, *Phytochemistry,* 2022, **197**, 113122.

32 L. Berstis, T. Elder, M. Crowley and G. Beckham, *ACS Sustain Chem Eng*, 2016, **4**, 5327–5335.

33 L. Berstis, T. Elder, R. Dixon, M. Crowley and G. Beckham, *ACS Sustain Chem Eng*, 2021, **9**, 1518–1528.

34 T. Elder, L. Berstis, G. Beckham and M. Crowley, *ACS Sustain Chem Eng*, 2017, **5**, 7188–7194.

35 L. Berstis, T. Elder, R. Dixon, M. Crowley and G. T. Beckham, *ACS Sustain Chem Eng*, 2021, **9**, 1518–1528.

36 D. Valencia, D. Vega and J. Aburto, *Renew Energy*, 2024, **222**, 119979.

37 T. Azad, H. F. Torres, M. L. Auad, T. Elder and A. J. Adamczyk, *Phys Chem Chem Phys*, 2021, **23**, 20919–20935.

38 R. Parthasarathi, R. A. Romero, A. Redondo and S. Gnanakaran, *J Phys Chem Lett*, 2011, **2**, 2660–2666.

39 Spartan'24, Wavefunction Inc., Irvine, CA.

40 Gaussian 16, Revision C.01, E. S. M. J. Frisch, G. W. Trucks, H. B. Schlegel, V. B. M. A. Robb, J. R. Cheeseman, G. Scalmani, A. V. M. G. A. Petersson, H. Nakatsuji, X. Li, M. Caricato, H. P. H. J. Bloino, B. G. Janesko, R. Gomperts, B. Mennucci, D. W.-Y. J. V. Ortiz, A. F. Izmaylov, J. L. Sonnenberg, A. P. F. Ding, F. Lipparini, F. Egidi, J. Goings, B. Peng, N. R. T. Henderson, D. Ranasinghe, V. G. Zakrzewski, J. Gao, R. F. G. Zheng, W. Liang, M. Hada, M. Ehara, K. Toyota, H. N. J. Hasegawa, M. Ishida, T. Nakajima, Y. Honda, O. Kitao, J. E. P. T. Vreven, K. Throssell, J. A. Montgomery, Jr., K. N. K. F. Ogliaro, M. J. Bearpark, J. J. Heyd, E. N. Brothers, J. N. V. N. Staroverov, T. A. Keith, R. Kobayashi, S. S. I. K. Raghavachari, A. P. Rendell, J. C. Burant, R. C. J. Tomasi, M. Cossi, J. M. Millam, M. Klene, C. Adamo, O. F. J. W. Ochterski, R. L. Martin, K. Morokuma O. Farkas, J. B. Foresman, and D. J. Fox, Gaussian, Inc., Wallingford CT, 2019.

The data supporting this article, cartesian coordinates for the lignin-carbohydrate complexes, have been included as part of the Supplementary Information